COMBINING CHEMISTRY AND ARTISTRY: SYNTHESIS AND IDENTIFICATION OF ARTISTIC COPPER PATINAS USING RAMAN SPECTROSCOPY

C. Drysdale
Breck School, Minneapolis, MN

The purpose of this study was to gain insight into the chemistry of artistic patination, with specific goals of identifying and characterizing synthetic patinas realized from artistic recipes. Six copper patinas (A-F) were synthesized using recipes obtained from artist's forums and blogs, You-tube videos, and do-it-yourself patination guides. Chemical composition of the resulting patinas was found with polarized light microscopy, regular light microscopy, and Raman spectroscopy. Patina A was identified as cupric sulfide (CuS), Patina B as gerhardtite ($Cu_2(NO_3)(OH)_3$), Patina C as a combination of gerhardtite and clinoatacamite ($Cu_2(OH)_3Cl$), and Patina E as basic cupric acetate. Though Patinas D and F were not fully chemically identified, the results suggest that Patina D is likely a form of cupric hydroxide, and Patina F is likely a form of cuprous oxide. Results will be used to develop scientifically based copper patina recipes and techniques, which will ultimately be compiled into a reference guide for use by artists.

Keywords: Copper, patina, Raman spectroscopy, polarized light microscopy, Becke line tests

Funding for materials and supplies came from Hamline University and Breck School.

This paper received a 2014 Minnesota Academy of Science STEM Communicator Award. The judging process for this award satisfied the function of manuscript review.

INTRODUCTION

The green coloration on the Statue of Liberty or on an old penny is known as a copper patina. A copper patina forms as a result of oxidation/reduction reactions primarily between elemental copper and oxygen, with variations resulting from temperature, moisture, and salinity conditions, as well as pollutants in the atmosphere[1]. In fact, even proximity to urban or marine settings can influence patina formation. Depending on exposure conditions, patinas vary anywhere in color from red, green, blue, brown, or black[2].

For aesthetic reasons, a number of artists use finishes on their work that imitate the appearance of natural patinas. These synthetic patinas are sometimes simulated using paint or bottled kits, but typically they are created by applying chemicals at high temperatures[3]. Different chemical treatments can be used to produce a wide range of colors and textures, as demonstrated in work by contemporary artist Cheryl Safren. However, even experienced patina artists have difficulty controlling the patination process as slight variations in types of chemicals, concentration, temperature, and application methods used can dramatically alter the appearance of patinas[4]. Very little is known about the chemistry involved in artistic patination, and the topic has only been touched upon in the scientific literature. A thorough understanding of the chemistry involved in artistic patination is necessary before dependable recipes and techniques can be developed for use by artists. The purpose of this study was to gain insight into the chemistry of artistic patination, with specific goals of identifying and characterizing synthetic patinas obtained from artistic recipes.

Work done by art conservationists was critical to this study, since natural copper patinas have been studied more extensively than artistic copper patinas. As the repair and preservation of patinated artworks necessitates an understanding of natural patination processes, art conservationists have employed

modern technologies to analyze copper patinas, including X-ray diffraction, scanning electron microscopy, electron microprobe analysis, and Raman spectroscopy[1]. A study by Guadagnini *et al.*[5] used scanning electron microscopy and energy dispersive spectrometry to study the morphological and electrochemical properties of patinas formed on bronze artifacts. In a study by Hayez *et al.*[6], several artistic copper nitrate and copper chloride patinas were investigated using X-ray diffraction and Raman spectroscopy to distinguish authentic patinas from forgeries. More recently, a study by Ropret *et al.*[7] expanded on Hayez's work, analyzing artistic patinas before and after exposure to an outdoor environment. Although a few studies have successfully used Raman Spectroscopy to study artistic patinas, none have been carried out for the purpose of improving patina recipes and techniques. In addition, none of the patinas synthesized and analyzed in this work have been examined before.

Techniques used by art conservationists to characterize natural copper and bronze patinas can be applied to the study of artistic copper and bronze patinas. Of these techniques, polarized light microscopy, Becke line tests, and Raman spectroscopy are frequently used.

Polarized light microscopy is a contrast-enhancing technique commonly used by art conservationists, particularly in the study of minerals, such as patinas[1]. Polarized light microscopy is distinguished from regular light microscopy by use of two polarizers, termed polarizer and analyzer. Most substances cannot be visualized under cross-polarized light, but materials with directionally dependent optical properties can. These materials are classified as anisotropic, while substances that cannot be visualized under cross-polarized light are classified as isotropic. Most patinas are anisotropic in nature, with the exception of copper sulfide patinas[1]. For this reason, polarized light microscopy is an invaluable identification technique for the study of patinas. A second identification technique used is a Becke line test, which is a method for determining relative refractive index of two different materials. In this study, patina crystals were compared to mounting media with known refractive indices. Although index of refraction is a characteristic property, it is dependent on temperature and difficult to determine with a high degree of precision[8]. For this reason, measurements of index of refraction were coupled with observations of anisotropy, color, shape, and size, as well as analysis with Raman spectroscopy.

Of the three techniques used by art conservationists, Raman spectroscopy is of particular value because it measures vibrational frequencies at low wavenumbers (< 500 cm^{-1}), typical of metal-ligand bonds such as those found in patination products. Additionally, Raman spectroscopy is more sensitive than other vibrational spectroscopy methods, such as infrared spectroscopy. In the study presented here, Raman spectra were taken for all synthesized patinas. Raman spectra were also taken of patina recipe components to determine if new corrosion products were formed or if starting materials simply accumulated on surfaces of copper substrates. To identify unknown compounds in synthesized patinas, spectra of patinas were compared to spectra found in the literature.

MATERIALS AND METHODS

Chemicals used to synthesize patinas were purchased from Sigma Aldrich (St. Louis, Missouri) and had a minimum purity of 99%, with the exception of artist-grade "liver of sulfur" (K_2S), which was purchased from the art supply store, *Cooltools*. A Brukker Senterra Raman Spectrometer equipped with a visible confocal microscope was used to collect Raman spectra.

Copper Preparation: Copper substrates were cut from sheets of 24-gauge copper (minimum purity 99.9%) into 3 x 3 cm squares. Substrates were then sanded for ten seconds with 120-grit sandpaper paper and degreased with acetone immediately preceding applications of patinas.

Patination: Patina application methods were adapted recipes found in artist's blogs and self-published do-it-yourself patination guides. (A complete list of blogs and artistic patina guides can be found in Table 1.). To synthesize patinas, three methods were chosen: boiling immersion, direct heat, and fume.

Table 1. Sources for patina recipes.

Patina	Recipe Source
A	Hodgepodgerie. Liver of Sulfur Patina. http://www.hodgepodgerie.com/liver-of-sulfur-patina.html
B	Frei, O. Cupric Nitrate Patination of Metals. *Ganoksin Jewelry Making*. http://www.ganoksin.com/borisat/nenam/cupric.htm
C	Edge, M. S. *The Art of Patinas*. Springfield: Michael S. Edge, 1990. .
D	Appalachian State University. Patina Recipes. http://www1.appstate.edu/~curtincm/sculpture/recipe/patina.pdf
E	Klingenberg, R. Vinger and Salt Patina. http://jewelrymakingjournal.com/vinegar-and-salt-patina/
F	The Science Company. Deep Rust Red Patina. http://www.sciencecompany.com/-W12C672.aspx#17

These methods were chosen because they are commonly used by artists and were easily translated into a lab environment. In the boiling immersion method, copper substrates were submerged in a boiling solution of chemicals until substrate surfaces developed color. In the direct heat method, copper substrates were directly heated on a hot plate before patina application. Once substrate began to turn bright orange, a layer of patina solution was applied with a paintbrush, alternating layers of patina solution with heating until a thick patina layer was developed. (Artists typically use a handheld propane or butane torch as a heat source; however, in this work a hot plate was used for safer, more controlled conditions.) In the fume method, copper substrates were placed into a sealed container with cotton soaked in chemical solution and allowed to sit for two days. Table 2 shows components, methods, and application techniques used in the three patination methods described above. After patina applications, all patinated copper substrates were rinsed with distilled, deionized water (ddH_2O) and allowed to air dry.

Patina Identification:

Polarized Light Microscopy with Becke Line Tests: Patinas were scraped off of copper samples, placed on microscope slides, and mounted in Cargille Meltmount mounting media. Color and crystallinity of patina crystals were determined. To determine if patinas were isotropic or anisotropic, slides were viewed using a polarized light microscope with the polarizer and analyzer oriented at right angles in the optical path. The refractive indices of patinas were measured using a succession of Becke line tests. The microscope stage was lowered, and the movement of the Becke Line (a halo of light on the periphery of the patina crystal) was observed. If the refractive index of the patina was greater than that of the mounting media, the Becke line moved towards the patina crystal, and visa versa. The Becke line test was repeated using standardized mounting media of refractive indices ranging from 1.4600-1.7000 RI.

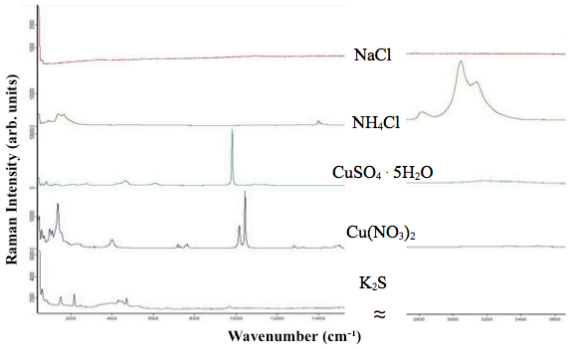

Figure 1. Raman spectra of patina recipe components: NaCl, NH_4Cl, $CuSO_4 \bullet 5H_2O$, $Cu(NO_3)_2$, K_2S

Raman Analysis: Raman spectra were collected on visually different regions of patina surfaces using a 20x objective lens and 785 and 532-nm lasers at 30-60 second integration times, and 10-50 mW power. Spectra were recorded from 0 cm^{-1} to 4000 cm^{-1}. To differentiate recipe components and reaction products, spectra were also taken of initial recipe components. (Spectra of recipe components can be found in Figure 1, and a complete list of peaks present in these spectra can be found in Table 3. No baseline subtraction or smoothing operation was applied to the spectra presented here.)

To identify compounds present in synthesized patinas, spectra of patinas were compared to reference spectra found in Frost *et al*.[9] of copper compounds associated with naturally occurring patinas. Relative intensities of patina spectra peaks were classified as very strong (vw), strong (s), medium (m), weak (w), very weak (vw), and shoulder (sh).

Table 2. Description of patina recipe components, water content, method of application, and time/numbers of applications.

Recipe	Components	Water	Method	Application
A	0.25 g K_2S	100 mL	boiling immersion	5 sec
B	20.0 g $Cu(NO_3)_2 \cdot 3H_2O$	100 mL	direct heat	25 applications
C	20.0 g $Cu(NO_3)_2 \cdot 3H_2O$ + 20.0 g NaCl	100 mL	boiling immersion	15 min
D	25.0 mL $C_2H_4O_2$ (10% solution) + 1.0 g NaCl	NA	fume	48 hr
E	25.0 mL NH_4OH (50% solution) + 1.0 g NaCl	NA	fume	48 hr
F	2.5 g $CuSO_4 \cdot 5H_2O$ + 0.5 g NH_4Cl	100 mL	boiling immersion	15 min 10 min

Table 3. Peaks from Raman spectra of recipe components, NaCl, NH4Cl, CuSO4 • 5H2O, Cu(NO3)2, K2S, given in cm^{-1}. (m=medium, s=strong, w=weak, vs=very weak, sh=shoulder)

NaCl	NH_4Cl	$CuSO_4 \cdot 5H_20$	$Cu(NO_3)_2 \cdot 3H_2O$	K_2S
--	45 m	62 vw	45 m	61 m
	60 s	82 w	60 s	82 w
	91 w	107 vw	71 w	151 w
	111 vwsh	124 vw	98 m	218 w
	141 w	134 vw	137 s	245 vw
	168 vw	196 vwsh	156 msh	397 vw
	193 wsh	205 vwsh	174 wsh	431 w
	339 w	213 vw	211 vwsh	435 wsh
	498 w	225 vwsh	220 vw	445 wsh
	1090 w	240 vwsh	236 vw	449 w
	1325 w	246 vw	244 vwsh	471 w
	1400 w	253 vwsh	399 w	290 vw
	1411 vwsh	262 vwsh	718 vw	497 vw
	1423 vwsh	278 vw	729 vw	519 vwsh
	1432 vwsh	330 vw	755 vw	524 vwsh
	2818 w	422 vwsh	764 vw	528 vwsh
	3045 vs	444 vwsh	1017 m	614 vw
	3119 ssh	457 vwsh	1045 vs	665 vw
	2141 s	468 w	1281 vw	696 vw
	3357 wsh	609 vw	1324 vw	996 vw
		982 vs	1431 vw	1005 vw
		1095 vw	1491 vwsh	
		1143 vw	1502 vw	
		3195 w	3340 vw	
		3340 w	3488 vw	

RESULTS

Polarized / Regular Light Microscopy Observations: Table 4 shows that Patinas B-F were anisotropic. Only Patina A was isotropic. The refractive index of Patina E fell within the range of mounting media used (1.5300-1.5400), while refractive indices of patinas A, B, C, D, and F fell outside of the range. Patinas B, C, D, E, and F were crystalline, while patina A was not. Patinas B-E ranged in color from blue, green, to turquoise. Patina A was black. (Photos of patinas are provided in Figure 2, with patinas viewed under a light microscope at 20X in Figure 3. Results obtained with polarized/regular light microscopy for recipe components can be found in Table 5.)

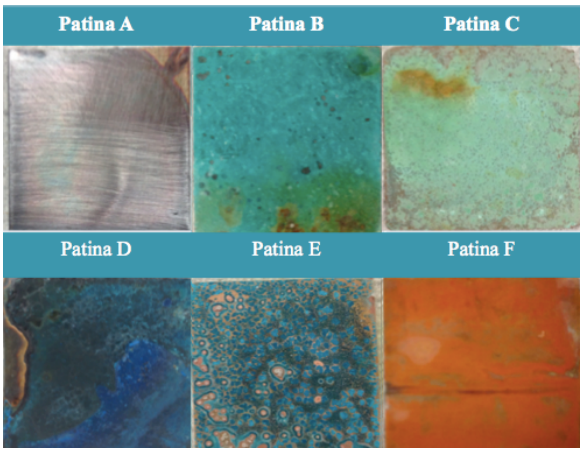

Figure 2. Patinas A-F

Raman Spectra: The peaks observed in the spectra of Patinas A-F are provided in Table 6. The spectrum of Patina A did not display Raman peaks. The clearest spectrum of Patina B was achieved with a 520 nm laser, 10 mW power, and 30 s integration time. A strong peak was observed at 1047 cm-1, which corresponds to a nitrate symmetric stretch.

The two peaks at 3479 and 3544 cm^{-1} were attributed to hydroxide stretching, and peaks observed in the lower region from 100-400 cm^{-1} were attributed to lattice vibrations (Figure 4). When peaks in the spectrum of Patina B were compared to a reference

Table 4. Components, anisotropy, refractive index, color, crystallinity, and chemical identification for patinas A-F.

Patina	Components	Anisotropy	R.I.	Color	Crystallinity	Identification
A	K_2S	Isotropic	< 1.4600	Black	Non-crystalline	CuS
B	$Cu(NO_3)_2 \cdot 3H_2O$	Anisotropic	> 1.7000	Turquoise	Crystalline	$Cu_2(NO_3)(OH)_3$
C	$Cu(NO_3)_2 \cdot 3H_2O$ + NaCl	Anisotropic	> 1.7000	Light turquoise	Crystalline	$Cu_2(NO_3)(OH)_3$, $Cu_2(OH)_3Cl$
D	NH_4OH + NaCl	Anisotropic	> 1.7000	Bright blue	Crystalline	Unknown
E	$C_2H_4O_2$ + NaCl	Anisotropic	1.5300 < x < 1.5400	Turquoise	Crystalline	$Cu(CH_3COO)_2 \cdot Cu(OH)_2 \cdot H_2O$
F	$CuSO_4 \cdot 5H2O$ + NH_4Cl	Anisotropic	< 1.4600	Dull red	Crystalline	Unknown

Table 5. Anisotropy, refractive index (RI), color, and crystallinity for patina components

Component	Anisotropy	R.I.	Color	Crystallinity
$CuSO_4 \cdot 5H_2O$	Anisotropic	1.514	Bright blue	Crystalline
$Cu(NO_3)_2 \cdot 3H_2O$	Anisotropic	1.744	Bright turquoise	Crystalline
NaCl	Isotropic	1.544	White	Crystalline, cubic
NH_4Cl	Isotropic	1.642	White	Crystalline, cubic

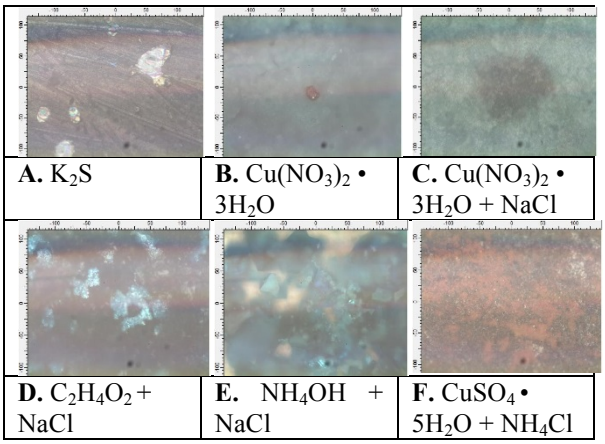

Figure 3. Photographs of Patinas (A-F) taken at 20X magnification.

for the mineral gerhardtite (Cu2(NO3)(OH)3), a strong similarity was observed. A direct peak comparison is provided in Table 7.

The clearest signal for Patina C was achieved with a 520 nm excitation line, 10 mW power, and 30 sec integration time. Different spectra were observed on the dark green regions (Fig. 5a) and light green regions (Fig. 5b) of the patina surface. A very strong band at 1068 cm^{-1}, corresponding to the nitrate symmetric stretch, was observed in the spectrum of

Table 6. Peaks observed in spectra of all patinas, given in cm^{-1}

A	B	C	D	E	F
—	62 s	60 w	60 vw	62 s	60 vw
	91 w	72 vwsh	92 vw	71 m	71 vw
	105 vw	76 vwsh	215 vw	91 s	94 vw
	114 vw	83 vwsh	286 m	98 m	107 vw
	125 vw	91 vwsh	444 vwsh	106 m	148 vw
	132 vw	96 vw	460 vwsh	126 msh	187 vwsh
	149 vwsh	104 vw	487 s	141 m	197 vwsh
	160 w	118 w	879 vw	181 wsh	209 vwsh
	184 vw	127 vwsh	952 vw	184 wsh	217 vw
	258 w	142 vw	3310 w	213 m	425 vw
	276 vw	151 vwsh	3553 s	224 m	631 vw
	333 vw	174 vw		231 m	802 vw
	407 vw	151 vwsh		253 w	913 vw
	455 vw	174 vw		266 w	1174 vw
	471 vwsh	250 vw		297 msh	1181 vwsh
	500 vw	268 vw		320 vs	1367 vwsh
	663 vw	277 vw		685 vwsh	1374 vw
	708 vw	358 vw		702 m	1378 vwsh
	719 vw	363 vw		939 wsh	1385 vwsh
	1028 vwsh	400 vw		948 vs	1397 vwsh
	1047 vs	449 vw		1360 vw	1444 vw
	1301 vwsh	455 vwsh		1412 vwsh	1484 vw
	1322 w	510 vwsh		1415 w	
	1426 vw	513 w		1420 wsh	
		895 vw		1440 w	
	3479 vw	973 vw		1444 wsh	
	3544 w	1052 vw		1449 wsh	
		3320 wsh		2940 m	
		3351 w		2980 vw	
		3435 wsh		3022 vw	
		3439 w			

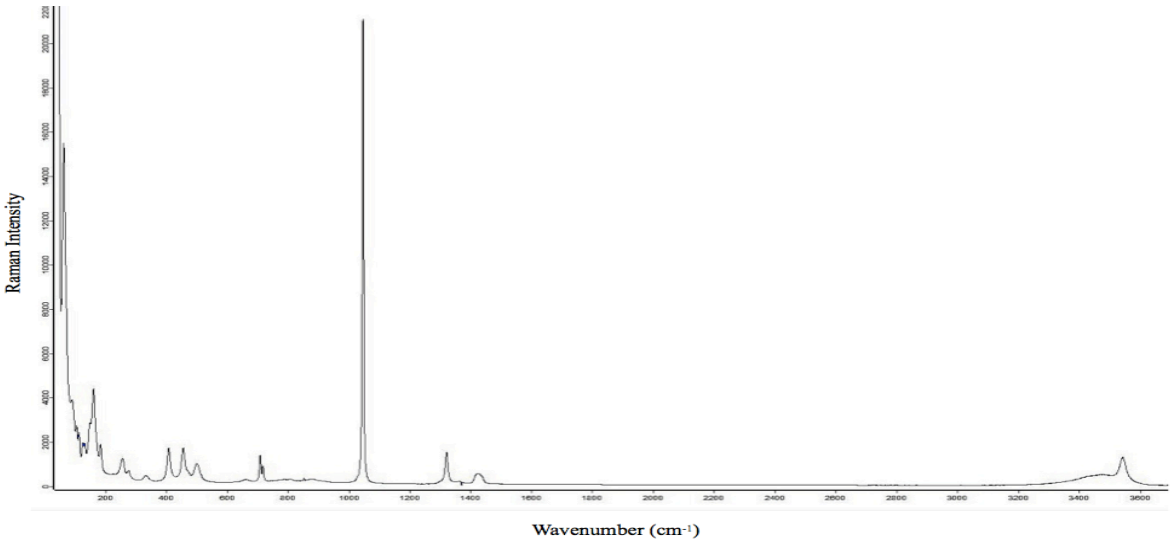

Figure 4. Raman spectrum of patina B. Peaks observed at 62 (s), 91 (w), 105 (vw), 114 (vw), 125 (vw), 132 (vw), 149 (vwsh), 160 (w), 184 (vw), 258 (w), 276 (vw), 333 (vw), 407 (vw), 455 (vw), 471 (vwsh), 500 (vw), 663 (vw), 708 (vw), 719 (vw) 1028 (vwsh), 1047 (vs), 1301 (vwsh), 1322 (w), 1426 (vw), 3479 (vw), and 3544 (w) cm^{-1}.

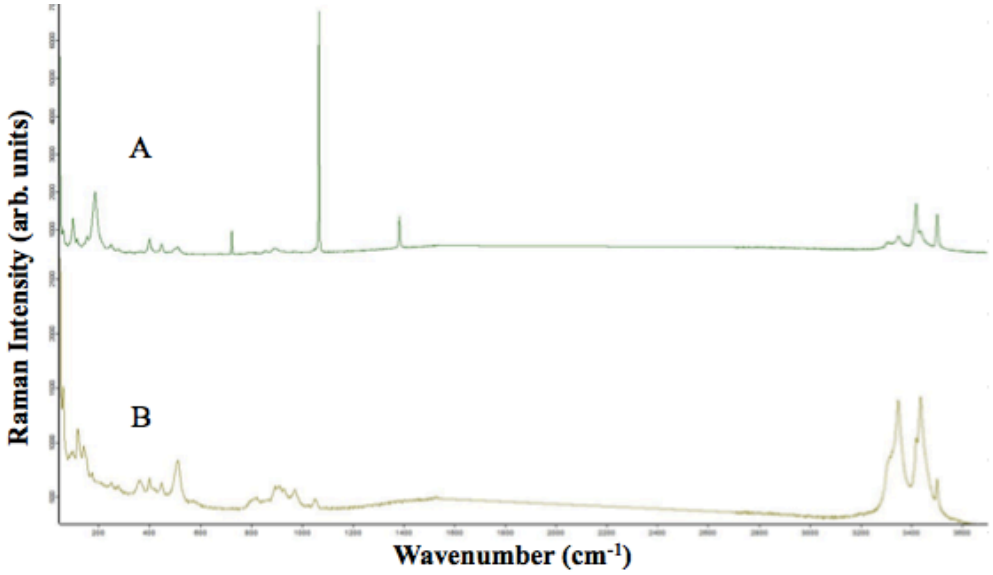

Figure 5. Raman spectrum of dark green region (A) and light green region (B) for Patina C. On dark green region peaks were observed at 60 (w), 72 (vwsh), 76 (vwsh), 85 (vwsh), 99 (w), 116 (vw), 141 (vw), 155 (vw), 177 (vwsh), 186 (m), 250 (w), 277 (vw), 280 (vw), 322 (vw), 363 (vw), 400 (w), 449 (w), 498 (wsh), 511 (w), 724 (w), 861 (vw), 895 (vw), 1052 (vwsh), 1068 (vs), 3310 (w), 3352 (w), 3436 (wsh), 3439 (w) cm^{-1}. On light green region peaks were observed at 60 (w), 72 (vwsh), 76 (vwsh), 83 (vwsh), 91 (vwsh), 96 (vw), 104 (vw), 118 (w), 127 (vwsh), 142 (vw), 151 (vwsh), 174 (vw), 250 (vw), 268 (vw), 277 (vw), 358 (vw), 363 (vw), 400 (vw), 449 (vw), 455 (vwsh), 510 (vwsh), 513 (w), 895 (vw), 973 (vw), 1052 (vw), 3320 (wsh), and 3351 (w) cm^{-1}

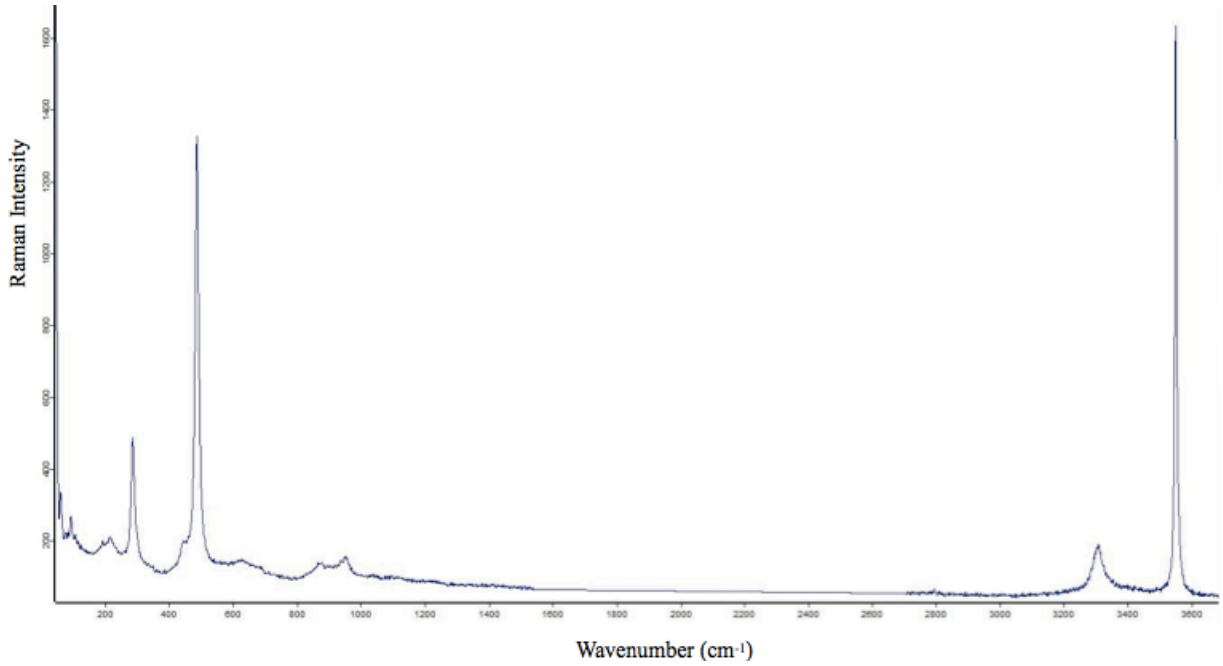

Figure 6. Raman Spectrum of Patina D. Peaks were observed at: 60 (vw), 92 (vw), 215 (vw), 286 (m), 444 (vwsh), 460 (vwsh), 487 (s), 879 (vw), 952 (vw), 3310 (w), and 3553 (s) cm^{-1}

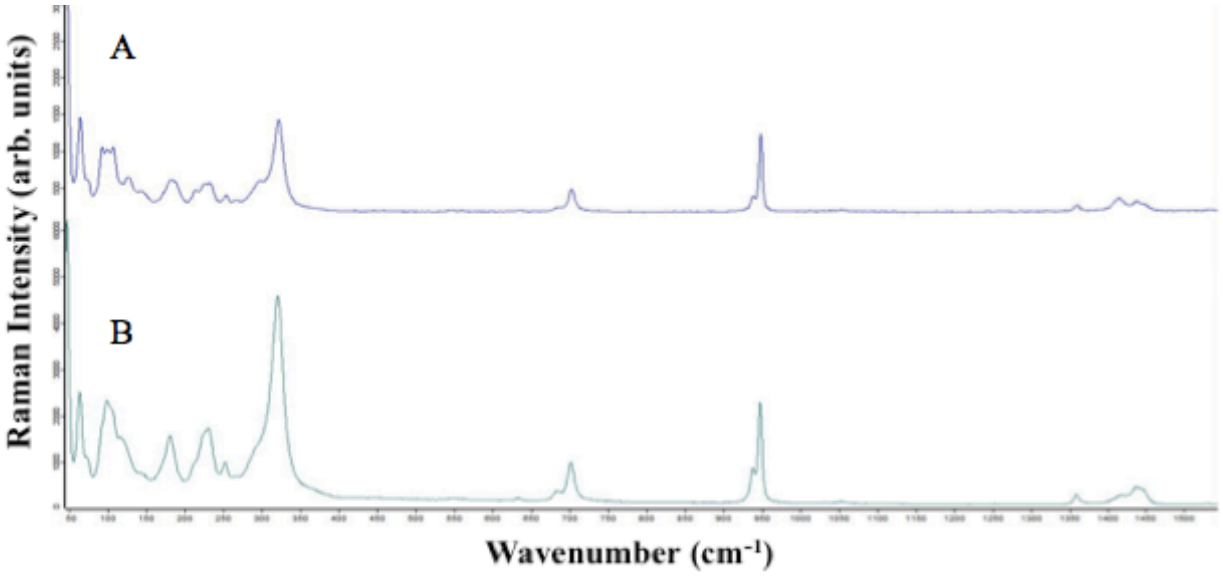

Figure 7. Spectrum of Patina E (A) and cupric acetate (B). Peaks were observed at 62 (s), 71 (m), 91 (s), 98 (m), 106 (m), 126 (msh), 141 (m), 181 (wsh), 184 (wsh), 213 (m), 224 (m), 231 (m), 253 (w), 266 (w), 297 (msh), 320 (vs), 685 (vwsh), 702 (m), 939 (wsh), 948 (vs), 1360 (vw), 1412 (vwsh), 1415 (w), 1420 (wsh), 1440 (w), 1444 (wsh), 1449 (wsh), 2940 (m), and 2980 (vw) cm^{-1}

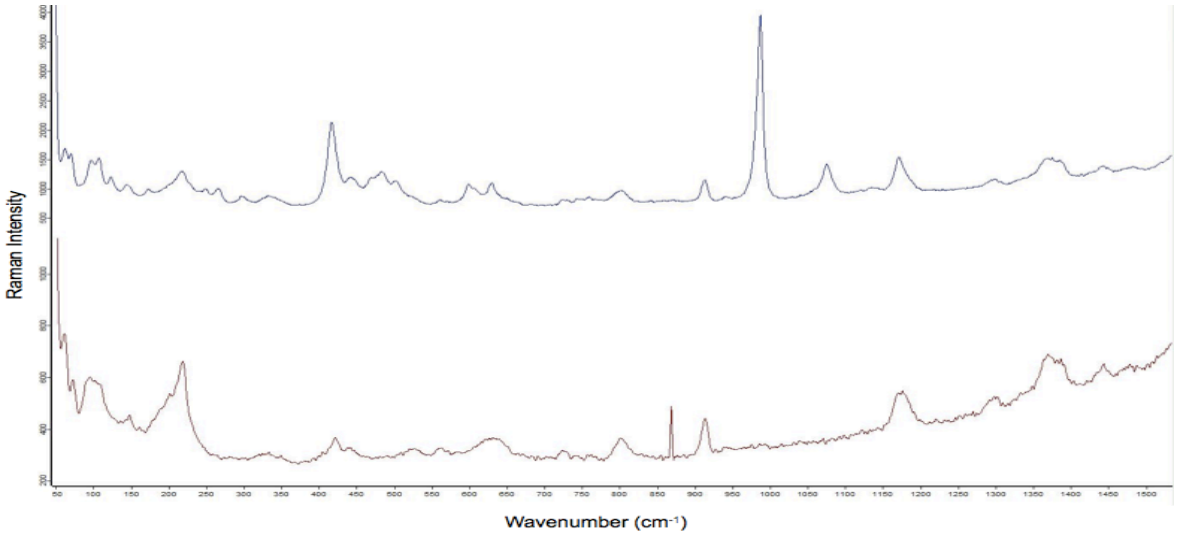

Figure 8. Spectrum of Patina F. On red region peaks observed at 60 (vw), 71 (vw), 94 (vw), 107 (vw), 148 (vw), 187 (vwsh), 197 (vwsh), 209 (vwsh), 217 (vw), 425 (vw), 631 (vw), 802 (vw), 913 (vw), 1174 (vw), 1181 (vwsh), 1367 (vwsh), 1374 (vw), 1378 (vwsh), 1385 (vwsh), 1397 (vwsh), 1444 (vw), 1484 (vw) cm^{-1}. On blue region peaks observed at 61 (m), 69 (msh), 97 (m), 106 (m), 122 (w), 143 (w), 172 (w), 209 (w), 217 (m), 228 (wsh), 248 (w), 268 (w), 296 (w), 325 (wsh), 332 (w), 341 (wsh), 415 (s), 441 (m), 448 (msh), 468 (m), 477 (msh), 483 (m), 502 (m), 522 (wsh), 560 (vw), 571 (vw), 598 (w), 607 (wsh), 631 (w), 801 (w), 913 (w), 987 (vs), 1172 (w), 1369 (w), 1384 (w), 1414 (vw), 1443 (vw), and 1484 (vw) cm^{-1}

the dark green region but not in the spectrum of the light green region. Both spectra displayed multiple peaks in the hydroxide stretching region, but with varying intensities. As recipe components included copper nitrate and sodium chloride, it is likely that the dark green spectrum corresponds to a nitrate-type patina and the light green spectrum to a chloride-type patina. When the spectrum of the dark green region was compared to a reference for the copper nitrate gerhardtite (Cu2(NO3)(OH)3), a strong similarity was observed. When the spectrum of the light green region was compared to a reference for the copper chloride clinoatacamite (Cu2(OH)3Cl), a strong similarity was observed. A direct comparison peak comparison is provided in Table 7.

The clearest signal for Patina D was achieved with a 520 nm excitation line, 10 mW power, and 30 sec integration time. The four most intense peaks in the spectra occurred at 286, 487, 3310, and 3553 cm^{-1}. The peak at 487 cm^{-1} corresponds to the copper oxide stretching mode, and the peaks at 3310 and 3553 cm^{-1} correspond to the hydroxide stretching mode, indicating the presence of a copper compound with at least one hydroxide group (Figure 6.). The spectrum did not match any published reference peaks.

The clearest signal for Patina E was achieved with a 520 nm laser and 10 mW power at 30 sec integration time. Major peaks at 98, 181, 231, 253, 320, 702, 939, 948, 1360, 1415, 1440, and 2940 cm^{-1} observed in Patina E were also present in the spectrum of cupric acetate with a 0-3 cm^{-1} allowance (Figure 7.). A direct peak-by-peak comparison is provided in Table 8.

The clearest signal for Patina F was achieved with a 520 nm excitation line, 30 sec integration time, and 10 mW power. Two different spectra were observed on red and blue regions of patina surface (Figure 8.). Neither spectrum matched any reference peaks, but the peaks at 441, 448, 468, 913, and 982 cm^{-1} in the blue spectrum match those found in the spectrum of copper sulfate.

Table 7. Peaks observed in spectra of copper nitrate patinas (B,C) and reference for gerhardtite ($Cu_2(NO_3)(OH)_3$) and clinoatacamite ($Cu_2(OH)_3Cl$). A strong similarity is found between Patina B and gerhardtite, and between Patina C and clinoatacamite. Peaks given in cm^{-1}

Patina B	Patina C (light green)	Patina C (dark green)	Gerhardtite [4]	Clinoatacamite [4]
62 s	60 w	60 w		
91 w	72 vwsh	72 vwsh		
105 vw	76 vwsh	76 vwsh		
114 vw	83 vwsh	85 vwsh		
125 vw	91 vwsh	99 w		
132 vw	96 vw	116 vw	132	
149 vwsh	104 vw	141 vw	149	
160 w	118 w	155 vw	165	118
184 vw	127 vwsh	177 vwsh	186	
258 w	142 vw	186 m	213	142
276 vw	151 vwsh	250 w	258	165
333 vw	174 vw	277 vw	279	183
407 vw	250 vw	280 vw	336	193
455 vw	268 vw	322 vw	410	206
471 vwsh	277 vw	363 vw	423	256
500 vw	358 vw	400 w	437	
663 vw	363 vw	449 w	458	364
708 vw	400 vw	498 wsh	474	420
719 vw	449 vw	511 w	503	445
1028 vwsh	455 vwsh	724 w	668	511
1047 vs	510 vwsh	861 vw	711	576
1301 vwsh	513 w	895 vw	720	799
1322 w	895 vw	1052 vwsh	805	866
1426 vw	973 vw	1068 vs	887	892
	1052 vw		1024	927
3479 vw		3310 w	1031	969
3544 w	3320 wsh	3352 w	1048	3314
	3351 w	3436 wsh	1052	3357
		3439 w	1324	3443
			1339	3475
			1417	
			1438	
			3391	
			3417	
			3477	
			3546	
			3556	

DISCUSSION

Patina A was black, non-crystalline, and isotropic - all qualities that are consistent with copper sulfides. No Raman signal in the spectrum of Patina A indicates the presence of a compound with less than three atoms, which are Raman inactive. The two-atom compound copper (I) sulfide (CuS) is a strong candidate considering the primary component used to synthesize Patina A was K_2S.

Patina B was turquoise, crystalline, and anisotropic. These qualities, as well as a refractive index of > 1.700, are consistent with the spectrum of cupric nitrate gerhardtite ($Cu_2(NO_3)(OH)_3$). The Raman spectrum of Patina B confirms this identification; there was a strong similarity between the reference spectrum for gerhardtite from Frost *et al.*[4] and the spectrum for Patina B. Remaining, unidentified peaks in the spectrum of Patina B could be due to the higher purity of the reference.

Table 8. Comparison of Patina E with reference spectrum obtained on cupric acetate ($Cu(CH_3COO)_2$). Peaks are given in cm^{-1}. A high similarity is observed between Patina E and cupric acetate.

Patina E	$Cu(CH_3COO)_2$
62 s	63 s
71 m	71 msh
91 s	98 s
98 m	105 ssh
106 m	116 msh
126 msh	140 wsh
141 m	180 m
181 wsh	
184 wsh	
213 m	214 wsh
224 m	224 msh
231 m	230 m
253 w	251 w
266 w	
297 msh	293 msh
320 vs	320 vs
685 vwsh	364 vwsh
702 m	633 vw
939 wsh	683 wsh
948 vs	702 m
1360 vw	938 msh
1412 vwsh	947 s
1415 w	1055 vw
1420 wsh	1359 w
1440 w	1418 wsh
1444 wsh	1439 w
1449 wsh	1446 wsh
2940 m	1531 vw
2980 vw	2940 w
3022 vw	2980 vw
	3022 w

Patina C was light turquoise, anisotropic, and crystalline, indicating the presence of cuprous chloride. The refractive index measured for Patina C (< 1.700) also supports this identification. When Patina C was viewed under a microscope using the 20X objective, two different regions were apparent: a dark turquoise region and a light turquoise region. Raman spectra collected for these regions were different, indicating formation of at least two compounds. A strong peak at 1068 cm^{-1} in the spectrum of the dark green region indicates the presence of cupric nitrate, which is notably absent

from the spectrum of the light green region. As recipe components included cupric nitrate and sodium chloride, it is likely that a nitrate-type patina was formed in addition to a chloride-type patina. Comparison to references from Frost *et al.*[9] allowed for specific identification: the spectrum of the dark green region of Patina C matched the spectrum of the cupric nitrate gerhardtite ($Cu_2(NO_3)(OH)_3$), and the spectrum of the light green region of Patina C matched the spectrum of the cupric chloride clinoatacamite ($Cu_2(OH)_3Cl$).

Patina D was bright blue, anisotropic, and crystalline. The strong blue color of Patina D indicates formation of a compound with the cupric ion. Raman spectrum of Patina D showed the presence of a hydroxyl group, which suggests a form of cupric hydroxide ($Cu(OH)_2$). However, the spectrum of Patina D did not match any considered reference.

Patina E was turquoise, anisotropic, and crystalline. These qualities are consistent with cupric acetate. The refractive index (1.5300-1.5400) indicated the formation of cupric acetate with specific stoichiometry of $Cu(CH_3COO)_2 \cdot Cu(OH)_2 \cdot H_2O$. Raman analysis confirmed this identification, as the spectrum of Patina E matched the spectrum collected for a sample of cupric acetate.

Patina F was dull red, anisotropic, and crystalline. The red color is indicative of a cupric oxide. The Raman spectrum did not match published references, although some peaks matched those found in the spectrum collected for cupric sulfate, which is likely a result of residue from patina application.

Of the six patinas synthesized in this work, Patinas A, B, C, and E were positively identified. Patinas D and F could not fully chemically identified. However, since they were synthesized using ingredients not commonly found in natural patinas, it is not surprising that they could not be matched to an equivalent naturally-occurring copper patina. Though Patinas D and F were not fully chemically identified, the results suggest that Patina D is likely a form of cupric hydroxide, and Patina F is likely a form of cuprous oxide.

Six artistic copper patinas were synthesized according to common artistic recipes obtained from artists' blogs and do-it-yourself patination guides. Analysis with Raman spectroscopy, polarized light microscopy, and regular light microscopy enabled the identification of four out of six synthesized patinas. Patina A was identified as cupric sulfite, Patina B as gerhardtite, Patina C as a combination of gerhardtite and clinoatacamite, and Patina E as cupric acetate. Although patinas D and F were not positively chemically identified, results suggest that patina D is a form of cupric hydroxide and Patina F is a form of cupric oxide.

To ensure reproducibility of results, the same recipes will be followed exactly and their resulting patinas analyzed with Raman Spectroscopy. Patinas realized from other artistic recipes will also be analyzed with polarized light microscopy, regular light microscopy, and Raman spectroscopy. In addition, analysis will be performed using X-ray diffraction (unavailable during the study presented here) to gather information about elemental composition of patinas. This work will contribute to development of scientifically based copper patina recipes and techniques that will ultimately be compiled into a reference guide for use by artists.

ACKNOWLEDGEMENTS

Dr. Deanna O'Donnell was the primary advisor for the project. She provided training on how to operate a Raman spectrometer. Dr. Glenn Harden gave training on the polarized light microscope. Ms. Lois Fruen and the Breck Advanced Science Research team read the paper and offered critique.

REFERENCES

1. Scott DA. Copper and Bronze in Art: Corrosion, Colorants, Conservation. Getty Conservation Institute, Los Angeles, CA, 2002, pp. 515.
2. Crescent City Copper. Why does copper turn green? http://www.crescentcitycopper.com/why-does-copper-turn-green.htm. 2010, July 31, 2013.
3. Cervin M. Chemistry on copper: The works of Cheryl Safren. http://www.copper.org/consumers/arts/2008/august/Cheryl_Safren.html. August, 2008, June 2, 2013.
4. Edge MS. The Art of Patinas for Bronze. Michael S. Edge, Springfield, OR, 1990, pp. 120.

5. Guadagnini L, Chiavari C, Martini C, Bernardi E, Morselli L, Tonelli D. The use of scanning electrochemical microscopy for the characterisation of patinas on copper alloys. *Electrochimica Acta*. 2011; 56(19): 6598-6606.
6. Hayez V, Costa V, Gillaume J, Terryn H, Hubin A. Micro Raman spectroscopy used for the study of corrosion products on copper alloys: Study of the chemical composition of artificial patinas used for restoration purposes. *Analyst*. 2005; 130(4): 550-556.
7. Ropret P, Kosec T. Raman investigation of artificial patinas on recent bronze – Part 1: Climatic chamber exposure. *Journal of Raman Spectroscopy*. 2012; 43(11):1578-1586.
8. Murphy DB, Salmon ED, Spring KR, Abramowitz M, Pluta M, Parry-Hill M, Sutter, RT, Davidson MW. Polarized light microscopy. http://www.olympusmicro.com/primer/techniques/polarized/polarizedhome.html. 2012, July 31, 2013.
9. Frost RL. Raman spectroscopy of selected copper minerals of significance in corrosion. *Spectrochimica acta. Part A: Molecular and Biomolecular Spectroscopy*. 2003; 59(6):1195-1204.